Electron transport and electrical properties in donor-acceptor copolymers:methanofullerene derivative blends

Y. R. CHEN, L. G. WANG[*], Y. GUO[*], L. ZHANG, Y. J. WANG
School of Electrical Engineering and Automation, Henan Polytechnic University, Jiaozuo, 454000, People's Republic of China

The bulk-heterojunction photovoltaic devices fabricated from blends of donor–acceptor (D–A) copolymers as electron donor and fullerene derivatives as electron acceptor have recently attracted considerable attention. In this paper, the electron transport and electrical properties in the blends of D–A copolymer DTS-HT-$C_0(F_2)$ and methanofullerene derivative $PC_{71}BM$ are investigated. From an analysis of the temperature dependence of the current density-voltage ($J - V$) characteristics of electron-only device based on the blends of DTS-HT-$C_0(F_2)$ and $PC_{71}BM$, it is found that consistent descriptions for the experimental measurements are obtained using both the improved extended Gaussian disorder model (IEGDM) and the extended correlated disorder model (ECDM), within which spatial correlations between the transport site energies are absent and are included, respectively. By comparing the model parameters with the typical values of organic materials, we view the more realistic intersite distance obtained using the IEGDM (3 nm) compared to the value obtained using the ECDM (0.78 nm) as an indication that in the DTS-HT-$C_0(F_2)$:$PC_{71}BM$ blends correlations between the transport site energies are absent. Furthermore, it is shown that the effective mobility in the DTS-HT-$C_0(F_2)$:$PC_{71}BM$ blends gradually increases with increasing temperature.

1. Introduction

Organic photovoltaics (OPVs) have been expected to provide next-generation energy sources because of their advantages like low cost, flexibility, low weight, and ease of processing [1-6]. The most prominent breakthrough for high-performance OPVs was based on the concept of a bulk-heterojunction (BHJ) structure in the organic active layer, which comprises a blend of a π-conjugated polymer as an electron donor (p-type) and a methanofullerene derivative as an electron acceptor (n-type) [7, 8]. To increase the power conversion efficiencies (PCEs), with regard to the electronic structure design, p-type materials should fulfill the following requirements: a reduced band gap to broaden the absorption range of solar light and a low-lying highest occupied molecular orbital (HOMO) energy level to increase the open-circuit voltage [8]. Therefore, the development of donor−acceptor (D−A) copolymers, which consist of alternating electron-rich and electron-deficient units, has become essential for efficient photovoltaic application, since it enables managing of light harvesting properties and energy level alignment [9-13]. Recently, Le et al. have reported that D−A copolymer DTS-$C_0(F_2)$ consisting of dithieno[3,2-b:2′,3′-d]silole (DTS) donor unit and fluorine-substituted naphtho[2,3-c]

thiophene-4,9-dione ($C_0(F_2)$) acceptor unit shows a PCE of 7.30% in combination with [6,6]-phenyl-C_{71}-butyric acid methyl ester ($PC_{71}BM$) as an n-type material [14]. However, investigation of the device operation revealed that the hole mobility of the DTS-HT-$C_0(F_2)$:$PC_{71}BM$ blend film is relatively low as compared to the electron mobility, which restricts the PCE to a moderate level. To enhance the hole-transporting characteristics, they further introduced a 3-hexylthiophene (HT) spacer unit between DTS and $C_0(F_2)$, resulting in a new D-A copolymer DTS-HT-$C_0(F_2)$. OPVs based on the blend of DTS-HT-$C_0(F_2)$ and $PC_{71}BM$ show an improved PCE of 9.12% [15]. But even so, OPV devices consisting of D-A copolymers with a higher PCE are still limited. To improve upon the performance of such devices, further understanding of the underlying physics of charge transport becomes important, as the mobility of the generated charge carriers is one of the key factors that decide how efficiently the charges can escape recombination and be extracted [16-19].

The charge carrier mobility in disordered organic semiconductors is determined by hopping between localized states. During the past two decades, various approaches were proposed to calculate the mobility function [20-25]. Seminal work by Bässler et al. used

Monte Carlo simulations, the random energies were described by a Gaussian density of states (DOS), leading to the Gaussian disorder model (GDM) [20], within which spatial correlations between the transport site energies are absent. Alternatively, it was suggested that the presence of dipole moments can give rise to spatial correlation between the site energies [21], leading to the correlated disorder model (CDM). Later, it was realized that, apart from the dependence of the mobility μ on the electric field E and temperature T, there is also a strong dependence on the carrier density p [22–25], giving rise to extended versions of the GDM and CDM, the EGDM [22] and ECDM [23]. For the GDM and CDM, key issues are the roles of the energetic disorder of the states where the charge carrier hopping occur, assuming a Gaussian density of state (DOS) with random and spatially correlated energetic disorder, respectively. Furthermore, it should be noted that the EGDM, only having non-Arrhenius temperature dependence, cannot well describe the charge transport at high carrier densities. In order to better describe the charge transport, we proposed an improved model within which the temperature dependence of the mobility based on both the non-Arrhenius temperature dependence and Arrhenius temperature dependence, leading to the improved extended Gaussian disorder model (IEGDM) [26].

In this paper, the electron transport and the possible presence of spatially correlated disorder in the DTS-HT-$C_0(F_2)$:$PC_{71}BM$ blends are investigated. Firstly, we perform a detailed analysis of the temperature dependence of the current density-voltage ($J-V$) characteristics of electron-only device based on the DTS-HT-$C_0(F_2)$:$PC_{71}BM$ blends by using the IEGDM and ECDM. It is found that an almost equally good fit to the $J(V)$ curves can be obtained using both the IEGDM and ECDM, but a more realistic value of the intersite distance is obtained within the IEGDM (3 nm) than that within the ECDM (0.78 nm), which indicate that in the blends of DTS-HT-$C_0(F_2)$:$PC_{71}BM$ spatially correlations between the transport site energies are absent. Subsequently, we calculate and analyze the variation of $J-V$ characteristics with the boundary carrier density and the distribution of carrier density and electric field with the distance from the interface of electron-only device based on the DTS-HT-$C_0(F_2)$:$PC_{71}BM$ blends. It is found that the effective mobility in the DTS-HT-$C_0(F_2)$:$PC_{71}BM$ blends gradually increases with increasing temperature. These systematic investigations will provide important insight for the development of high performance OPV devices based on D–A copolymers:methanofullerene derivative.

2. Models and methods

Based on numerical transport simulations accounting for hopping on a simple cubic lattice with uncorrelated Gaussian disorder, the extended Gaussian disorder model (EGDM) has been developed by Pasveer et al. [22]. To improve upon the applicable range of the EGDM, we proposed an improved mobility model (IEGDM) [26]. In particular, the dependence of the zero-field mobility on the carrier density p and temperature T is given by

$$\mu(T,p) = \mu_0(T)\exp[\frac{1}{2}(\hat{\sigma}^2 - \hat{\sigma})(2pa^3)^{\delta}], \quad (1a)$$

$$\mu_0(T) = \mu_0 c_1 \exp(c_2\hat{\sigma} - c_3\hat{\sigma}^2), \quad (1b)$$

$$\delta \equiv 2\frac{\ln(\hat{\sigma}^2 - \hat{\sigma}) - \ln(\ln 4)}{\hat{\sigma}^2}, \quad \mu_0 \equiv \frac{a^2 v_0 e}{\sigma}, \quad (1c)$$

with $c_1 = 0.48 \times 10^{-9}$, $c_2 = 0.80$, and $c_3 = 0.52$. Where $\mu_0(T)$ is the mobility in the limit of zero carrier density and zero electric field, $\hat{\sigma} \equiv \sigma/k_B T$ is the dimensionless disorder parameter, σ is the width of the Gaussian density of states (DOS), a is the lattice constant (intersite distance), e is the charge of the carriers, and v_0 is the attempt-to-hop frequency. The field dependence of the mobility is included via

$$\mu(T,p,E) = \mu(T,p)^{g(T,E)} \exp[c_4(g(T,E)-1)], \quad (2)$$

$$g(T,E) = [1 + c_5(Eea/\sigma)^2]^{-1/2}, \quad (3)$$

where $g(T,E)$ is a weak density dependent function, c_4 and c_5 are weak density dependent parameters, given by

$$c_4 = d_1 + d_2\ln(pa^3) \quad (4a)$$

$$c_5 = 1.16 + 0.09\ln(pa^3) \quad (4b)$$

$$d_1 = 28.7 - 36.3\hat{\sigma}^{-1} + 42.5\hat{\sigma}^{-2} \quad (5a)$$

$$d_2 = -0.38 + 0.19\hat{\sigma} + 0.03\hat{\sigma}^2 \quad (5b)$$

Bouhassoune et al. employed the same methodology as in EGDM, but for an energy landscape with Gaussian disorder σ that results from randomly oriented dipole moments of equal magnitude on all lattice sites, leading to the extended correlated disorder model (ECDM) [23], which can be described by the following expression:

$$\mu(T,p,E) = [(\mu_{low}(T,p,E))^{q(\hat{\sigma})} + (\mu_{high}(p,E))^{q(\hat{\sigma})}]^{1/q(\hat{\sigma})},$$
$$(6)$$

$$q(\hat{\sigma}) = 2.4/(1 - \hat{\sigma}), \quad (7)$$

with $\mu_{low}(T,p,E)$ the mobility in the low-field limit (the average reduced field $E_{red} = eaE/\sigma \leq 1$), and with $\mu_{high}(p,E)$ the mobility in the high-field limit (the average reduced field $E_{red} = eaE/\sigma \geq 1$).

$$\mu_{low}(T,p,E) = \mu_0(T)g(T,p)f(T,E,p) \quad (8)$$

where $g(T,p)$ and $f(T,E,p)$ are the dimensionless mobility enhancement functions. These functions can be written as follows:

$$\mu_0(T) = 1.0 \times 10^{-9}\,\mu_0 \exp(-0.29\hat{\sigma}^2), \qquad (9)$$

$$g(T,p) = \begin{cases} \exp[(0.25\hat{\sigma}^2 + 0.7\hat{\sigma})(2pa^3)^\delta], pa^3 < 0.025 \\ g(T, 0.025a^{-3}), pa^3 \geq 0.025 \end{cases}$$

$$(10)$$

$$\delta \equiv 2.3\,\frac{\ln(0.5\hat{\sigma}^2 + 1.4\hat{\sigma}) - 0.327}{\hat{\sigma}^2}, \qquad (11)$$

$$f(T, E_{red}, p) = \exp[h(E_{red})(1.05 - 1.2(pa^3)^{r(\hat{\sigma})})$$
$$(\hat{\sigma}^{3/2} - 2)(\sqrt{1 + 2E_{red}} - 1)] \qquad (12)$$

$$h(E_{red}) = 1, \quad r(\hat{\sigma}) = 0.7\hat{\sigma}^{-0.7}, \qquad (13)$$

within the very low-field, $0 \leq E_{red} < 0.16 \equiv E^*_{red}$, $h(E_{red})$ can be written as

$$h(E_{red}) = \begin{cases} \dfrac{4}{3}\dfrac{E_{red}}{E^*_{red}}, (E_{red} \leq E^*_{red}/2) \\ \left[1 - \dfrac{4}{3}\left(\dfrac{E_{red}}{E^*_{red}} - 1\right)^2\right], \left(E^*_{red}/2 \leq E_{red} \leq E^*_{red}\right) \end{cases} \qquad (14)$$

$$\mu_{high}(p, E) = \frac{2.06 \times 10^{-9}}{E_{red}}\mu_0(1 - pa^3). \qquad (15)$$

By using the above two mobility models, the $J-V$ characteristics of organic electron devices can be exactly calculated by numerically solving the following equations adopting a particular uneven discretization method introduced in our previous paper [27, 28].

$$J = p(x)e\mu(T, p(x), E(x))E(x), \qquad (16a)$$

$$\frac{dE}{dx} = \frac{e}{\varepsilon_0\varepsilon_r}p(x), \qquad (16b)$$

$$V = \int_0^L E(x)dx, \qquad (16c)$$

where x is the distance from the injecting electrode, L is the organic semiconductor layer thickness sandwiched between two electrodes, $\varepsilon_0\varepsilon_r$ is the permeability of the organic semiconductors.

3. Results and discussion

For a system with Gaussian disorder, the mobility characteristics can be described by both the IEGDM and ECDM, which only use three parameters: the width of the Gaussian density of states distribution σ, the intersite distance a, and a mobility prefactor μ_0. The σ mainly controls its temperature and carrier density dependence, a mainly affects its field dependence, and the mobility prefactor determines the magnitude of the

mobility. The solution of the coupled equations (Eq. (16)) with the above two models and the experimental J-V measurements from Ref. [15] for electron-only device based on the DTS-HT-C$_0$(F$_2$):PC$_{71}$BM blends with various temperatures are displayed in Figs. 1 and 2, respectively. It can be seen from the figures that the temperature dependent $J-V$ characteristics of electron-only device based on the DTS-HT-C$_0$(F$_2$):PC$_{71}$BM blends can be well described by both the IEGDM and ECDM using a single set of model parameters, $a = 3$ nm, $\sigma = 0.091$ eV, $\mu_0 = 240\,\mathrm{m^2/Vs}$ and $a = 0.78\,\mathrm{nm}$, $\sigma = 0.103\,\mathrm{eV}$, $\mu_0 = 710\,\mathrm{m^2/Vs}$, respectively. The key parameters in both the IEGDM and ECDM are the strength of the energetic disorder, quantified by the width of the DOS σ, and the average hopping site distance a. The optimal fit values of a as obtained from the IEGDM and ECDM are very different, viz. 3 nm and 0.78 nm, respectively. The value of a found for the IEGDM is very close to the typical value of fullerenes and their derivatives, slightly larger than the result reported by Eersel et al. for PCBM (2.54 nm) [29], and equal to the value obtained from the EGDM by Kotadiya et al. for ICBA (3.0 nm) [5]. However, the value of a found for the ECDM may be considered as unrealistically small. This suggests that in the DTS-HT-C$_0$(F$_2$):PC$_{71}$BM blends the energies of the sites in between which hopping takes place are uncorrelated. The values obtained for σ does not change this point of view. For disordered organic semiconductors, the Gaussian density of states σ is typically observed to fall in the range 0.06-0.16 eV, the optimal values of σ obtained within both models (0.091 eV for the IEGDM and 0.103 eV for the ECDM) are physically realistic.
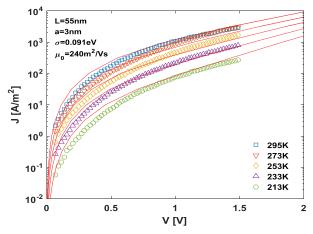

Fig. 1. Temperature dependent J-V characteristics of an electron-only device based on DTS-HT-C$_0$(F$_2$):PC$_{71}$BM blends with a layer thickness of 55 nm. Symbols are experimental data from Ref. [15]. Lines are the numerically calculated results based on the IEGDM
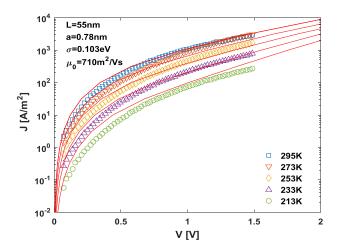
(color online)

Fig. 2. Temperature dependent J-V characteristics of an electron-only device based on DTS-HT-C$_0$(F$_2$):PC$_{71}$BM blends with a layer thickness of 55 nm. Symbols are experimental data from Ref. [15]. Lines are the numerically calculated results based on the ECDM (color online)

As a next step, we will perform a systematic study for electrical properties of the DTS-HT-C$_0$(F$_2$):PC$_{71}$BM blends by using the IEGDM and numerical method as described in section 2. The numerically calculated variations of $J-V$ characteristics with the boundary carrier concentration $p(0)$ for electron-only device based on DTS-HT-C$_0$(F$_2$):PC$_{71}$BM blends at various temperatures are plotted in Fig. 3. The figure shows that the voltage increases with increasing the current density, and the variation of voltage with $p(0)$ is dependent on the current density. In the density range of 10^{23}–10^{25} m^{-3}, the $V-p(0)$ curves are fairly flat, indicating that the voltage is almost independent of $p(0)$ and the $J-V$ characteristics are physically realistic in this region. Furthermore, it can be seen from the figure that in order to reach the same current density J at the same $p(0)$, the stronger electric field and the corresponding larger voltage are needed at 213 K than those at 295 K. This can be explained by the fact that the effective mobility as determined at 295 K is higher than that at 213 K.

The numerically calculated distribution of the carrier density and electric field as a function of the distance from the interface of electron-only device based on the DTS-HT-C$_0$(F$_2$):PC$_{71}$BM blends at various temperatures are plotted in Fig. 4. It is clear from the figure that the carrier density $p(x)$ is a decreasing function of the distance x, whereas the electric field $E(x)$ is an increasing function of the distance x. The decrease of the carrier density $p(x)$ for relatively large $p(0)$ is faster than that for relatively small $p(0)$. On the other hand, the increase of the electric field $E(x)$ for relatively large $p(0)$ is faster than that for relatively small $p(0)$. With the distance x increasing, $p(x)$ rapidly reaches saturation. The thickness of accumulation layer decreases with increasing $p(0)$.
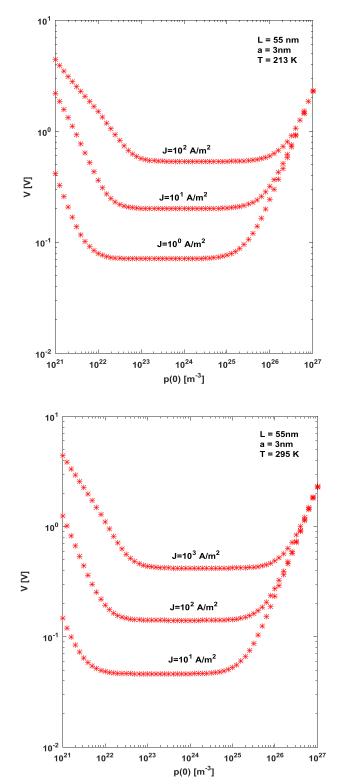

Fig. 3. Theoretical results of voltage versus the boundary carrier density of an electron-only device based on DTS-HT-C$_0$(F$_2$):PC$_{71}$BM blends at various temperatures (color online)

The variation tendency of carrier density $p(x)$ and electric field $E(x)$ with the distance x at 213 K is more obvious than that at 295 K, which further indicates

that the effective mobility at 295 K is higher than that at 213 K. Both the maximum of carrier concentration and the minimum of electric field appear near the interface of electron-only device based on DTS-HT-$C_0(F_2)$:$PC_{71}BM$ blends. As a result, the injection of carriers from the electrode into the DTS-HT-$C_0(F_2)$:$PC_{71}BM$ organic layer

leads to carriers accumulation near the interface and a decreasing function $p(x)$. The distribution of $p(x)$ leads to the variation of $E(x)$, and the carriers accumulation near the interface results in increasing function $E(x)$.
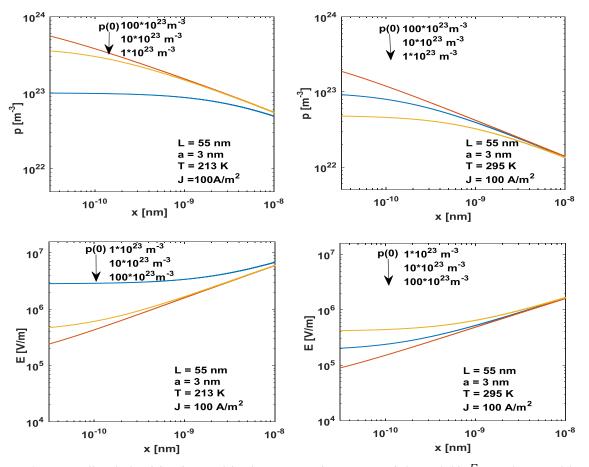

Fig. 4. Numerically calculated distribution of the charge carrier density p and electric field E as a function of the distance X in an electron-only device based on DTS-HT-$C_0(F_2)$:$PC_{71}BM$ blends at various temperatures (color online)

4. Summary and conclusions

In conclusion, the electron transport and the possible presence of spatially correlated disorder in the blends of D-A copolymer DTS-HT-$C_0(F_2)$ and methanofullerene derivative $PC_{71}BM$ are investigated. It is found that the temperature dependent $J-V$ characteristics of electron-only device based on DTS-HT-$C_0(F_2)$:$PC_{71}BM$ blends can be well described using both the IEGDM and ECDM, within which spatial correlations between the transport site energies are absent and are included, respectively. For the organic material studied, the intersite distance $a = 3$ nm is found for the IEGDM, whereas the value of a obtained for the ECDM is 0.78 nm. The intersite distance found using the IEGDM is very close to the typical value of fullerenes and their derivatives, whereas the value of a found for the ECDM may be considered as unrealistically small. This indicates that for the DTS-HT-$C_0(F_2)$:$PC_{71}BM$ blends

correlations between the site energies are absent. Furthermore, the effective mobility in DTS-HT-$C_0(F_2)$:$PC_{71}BM$ blends increases with increasing temperature. These results are useful to build up the quantitative organic device models and will provide important insight for the development of high performance OPV devices.

References

[1] G. Dennler, M. C. Scharber, C. J. Brabec, Adv. Mater. **21**, 1323 (2009).

[2] K. A. Mazzio, C. K. Luscombe, Chem. Soc. Rev. **44**, 78 (2015).

[3] G. J. Hedley, A. Ruseckas, I. D. W. Samuel, Chem. Rev. **117**, 796 (2017).

[4] Y. Ie, K. Morikawa, W. Zajaczkowski, W. Pisula, N. B. Kotadiya, G. A. H. Wetzelaer, P. W. M. Blom, Y. Aso, Adv. Energy Mater. **8**, 1702506 (2018).

[5] N. B. Kotadiya, P. W. M. Blom, G. A. H. Wetzelaer, Phys. Rev. Applied **11**, 024069 (2019).

[6] T. Upreti, Y. Wang, H. Zhang, D. Scheunemann, F. Gao, M. Kemerink, Phys. Rev. Applied **12**, 064039 (2019).

[7] G. Yu, J. Gao, J. C. Hummelen, F. Wudl, A. J. Heeger, Science **270**, 1789 (1995).

[8] A. J. Heeger, Adv. Mater. **26**, 10 (2014).

[9] Y. Li. Acc. Chem. Res. **45**, 723 (2012).

[10] Y. Ie, J. Huang, Y. Uetani, M. Karakawa, Y. Aso, Macromolecules **45**, 4564 (2012).

[11] J. S. Wu, S. W. Cheng, Y. J. Cheng, C. S. Hsu, Chem. Soc. Rev. **44**, 1113 (2015).

[12] J. Huang, Y. Ie, M. Karakawa, M. Saito, I. Osaka, Y. Aso, Chem. Mater. **26**, 6971 (2014).

[13] Y. Ie, Y. Aso, Polymer Journal **49**, 13 (2017).

[14] Y. Ie, K. Morikawa, M. Karakawa, N. B. Kotadiya, G. J. A. H. Wetzelaer, P. W. M. Blom, Y. Aso, J. Mater. Chem. A **5**, 19773 (2017).

[15] Y. Ie, K. Morikawa, W. Zajaczkowski, W. Pisula, N. B. Kotadiya, G. J. A. H. Wetzelaer, P. W. M. Blom, Y. Aso, Adv. Energy Mater. **8**, 1702506 (2018).

[16] C. Deibel, A. Wagenpfahl, V. Dyakonov, Phys. Status Solidi Rapid Res. Lett. **2**, 175 (2008).

[17] I. A. Howard, F. Etzold, F. Laquai, M. Kemerink, Adv. Energy Mater. **4**, 1301743 (2014).

[18] A. Melianas, V. Pranculis, A. Devižis, V. Gulbinas, O. Inganas, M. Kemerink, Adv. Funct. Mater. **24**, 4507 (2014).

[19] A. Melianas, F. Etzold, T. J. Savenije, F. Laquai, O. Inganas, M. Kemerink, Nat Commun. **6**, 8778 (2015).

[20] H. Bässler, Phys. Status Solidi B **175**, 15 (1993).

[21] Y. N. Gartstein, E. M. Conwell, Chem. Phys. Lett. **245**, 351 (1995).

[22] W. F. Pasveer, J. Cottaar, C. Tanase, R. Coehoorn, P. A. Bobbert, P. W. M. Blom, D. M. de Leeuw, M. A. J. Michels, Phys. Rev. Lett. **94**, 206601 (2005).

[23] M. Bouhassoune, S. L. M. van Mensfoort, P. A. Bobbert, R. Coehoorn, Org. Electron. **10**, 437 (2009).

[24] S. D. Baranovskii, Phys. Status Solidi A **215**, 1700676 (2018).

[25] N. Felekidis, A. Melianas, M. Kemerink, Org. Electron. **61**, 318 (2018).

[26] L. G. Wang, H. W. Zhang, X. L. Tang, C. H. Mu, Eur. Phys. J. B **74**, 1 (2010).

[27] L. G. Wang, H. W. Zhang, X. L. Tang, Y. Q. Song, Optoelectron. Adv. Mat. **5**, 263 (2011).

[28] M. L. Liu, L. G. Wang, J. Optoelectron. Adv. M. **19**(5-6), 406 (2017).

[29] H. van Eersel, R. A. J. Janssen, M. Kemerink, Adv. Funct. Mater. **22**, 2700 (2012).

_____

*Corresponding author: wangliguo@hpu.edu.cn，
guoyu@hpu.edu.cn